Protein Cell 2013, 4(9): 711–721
DOI 10.1007/s13238-013-3910-3

Protein & Cell

RESEARCH ARTICLE

ULK1 and JNK are involved in mitophagy incurred by LRRK2 G2019S expression

Yuangang Zhu*, Chunyan Wang*, Mei Yu, Jie Cui, Liang Liu, Zhiheng Xu✉

The National Key Laboratory of Molecular Developmental Biology, Institute of Genetics and Developmental Biology, Chinese Academy of Sciences, Beijing 100101, China
✉ Correspondence: zhxu@genetics.ac.cn
Received July 1, 2013 Accepted July 25, 2013

ABSTRACT

Mutations in *LRRK2* (Leucine rich repeat kinase 2) are a major cause of Parkinson's disease (PD). We and others reported recently that expression of the pathogenic gain-of-function mutant form of *LRRK2*, *LRRK2 G2019S*, induces mitochondrial fission in neurons through DLP1. Here we provide evidence that expression of *LRRK2 G2019S* stimulates mitochondria loss or mitophagy. We have characterized several LRRK2 interacting proteins and found that LRRK2 interacts with ULK1 which plays an essential role in autophagy. Knockdown of either ULK1 or DLP1 expression with shRNAs suppresses *LRRK2 G2019S* expression-induced mitochondrial clearance, suggesting that LRRK2 G2019S expression induces mitochondrial fission through DLP1 followed by mitophagy via an ULK1 dependent pathway. In addition to ULK1, we found that LRRK2 interacts with the endogenous MKK4/7, JIP3 and coordinates with them in the activation of JNK signaling. Interestingly, *LRRK2 G2019S*-induced loss of mitochondria can also be suppressed by 3 different JNK inhibitors, implying the involvement of the JNK pathway in the pathogenic mechanism of mutated LRRK2. Thus our findings may provide an insight into the complicated pathogenesis of PD as well as some clues to the development of novel therapeutic strategies.

KEYWORDS LRRK2, Parkinson's disease, mitophagy, ULK1, JNK, DLP1

INTRODUCTION

Mutations in leucine-rich repeat kinase 2 (LRRK2) can lead to autosomal dominant PD and are by far the most common cause of familial PD, accounting for as much as 40% of all cases in some populations and up to 5% of apparently sporadic cases (Kumari and Tan, 2009; Cookson, 2010). LRRK2 encodes a 2,527 aa protein containing several conserved domains including a leucine-rich repeat (LRR), a Roc-COR (C-terminal of Roc), a kinase, and a WD40 domain. The kinase domain of LRRK2 is homologous to that of the mixed-lineage kinases (MLKs) which we have shown previously to play an important role in neuronal cell death (Xu et al., 2001, 2003, 2005). The most prevalent mutation of LRRK2, G2019S, is associated with an increase kinase activity and neuronal cell death, indicating a gain-of-function mechanism for LRRK2-induced neuron loss in PD (West et al., 2005; Greggio et al., 2006; Cookson, 2010; Cui et al., 2011).

More and more studies have revealed a role of mitochondrial dysfunction in PD (Saha et al., 2009; Exner et al., 2012). We and others have shown recently that expression of LRRK2 G2019S may induce neuronal dysfunction by disturbing mitochondrial fission/fusion dynamics and function through DLP1 (Dynamin like protein 1) (Niu et al., 2012; Wang et al., 2012). Despite some discrepancy, there are several indications of the involvement of LRRK2 in the regulation of autophagy, the cell self-digestion and neuroprotective process (Chen and Chan, 2009; Ramonet et al., 2011; Tamura et al., 2011; Wang et al., 2012). Interestingly, disruption of autophagy leads to dopaminergic axon and dendrite degeneration and promotes presynaptic accumulation of α-synuclein and LRRK2 in the brain (Friedman et al., 2012). Whether LRRK2 G2019S-induced mitochondria fission would lead to subsequent autophagy and mitochondria clearance in neuron and what is the underlying mechanism remain unclear.

JNK represents one of the major signaling pathways implicated in PD pathogenesis since increased JNK activity and its association of mitochondria dysfunction has been reported in various neurotoxin and genetic PD animal models (For review, see Jankowski, 2007; Berwick and Harvey, 2011; Santos and

*These authors contributed equally to the work.

© Higher Education Press and Springer-Verlag Berlin Heidelberg 2013

Cardoso, 2012). Different components of the JNK pathway including MKKs (mitogen-activated protein kinase kinases), JNKs (c-Jun N-terminal kinases) and JIPs (JNK-interacting proteins) have been shown to interact with LRRK2 in overexpression or *in vitro* system (For review, see Kuan and Burke, 2005; Jankowski, 2007; Berwick and Harvey, 2011;). A recent study has found that JNK activity is increased in the substantia nigra of LRRK2 G2019S transgenic mice (Chen et al., 2012). Although expression of LRRK2 has been shown to be able to phosphorylate MKK4 and MKK7, which act upstream of the JNK (Gloeckner et al., 2009), the effect of LRRK2 on JNK activity is still uncertain (Berwick and Harvey, 2011).

Uncoordinated family member (unc) 51-like kinase 1(ULK1), a serine threonine kinase with homology to yeast Atg1, plays an essential role in the initiation of autophagy (Kundu et al., 2008; Egan et al., 2011; Tamura et al., 2011; Itakura et al., 2012). ULK1 can interact with different proteins to form a complex (the ULK1 complex) and this complex plays a crucial role in starvation-induced autophagy, integrating signals from upstream sensors such as mTOR and AMPK and transducing them downstream to govern autophagosome formation (Mizushima, 2010; Egan et al., 2011; Tamura et al., 2011). In addition, the ULK1 complex has been recognized recently as an important regulator of mitochondrial clearance or mitophagy, including targetting depolarized mitochondria at the initial stages of Parkin-mediated mitophagy (Kundu et al., 2008; Egan et al., 2011; Itakura et al., 2012).

In this study, we have screened and confirmed more LRRK2-interacting proteins through yeast two hybrid and co-immunoprecipitation. We found that ULK1 interacts with LRRK2 and plays an essential role in LRRK2 G2019S-induced mitochondria clearance. In addition, we confirmed that several components of the JNK pathway interact with LRRK2 in the brain of LRRK2 G2019S transgenic mice and expression of LRRK2 induces the activation of JNK. Interestingly, LRRK2 G2019S-induced mitochondrial clearance can also be suppressed by different JNK inhibitors.

RESULTS

LRRK2 interacts with ULK1

In order to elucidate the function of LRRK2, we performed yeast two-hybrid screen using 3 different LRRK2 fragments (LRRK2-AL, LRRK2-RC, LRRK2-MW) as baits to identify novel LRRK2 interacting proteins (Fig. 1A). When the C-terminal part of LRRK2 (LRRK2-MW) including the MAPKKK and WD40 domains (5341–7584 bp) of LRRK2 were used as a bait (Fig. 1A), three strong positive clones were observed from a total of ~3 × 10^6 independent transformants from a mouse brain library analyzed (data not shown). Sequence analysis revealed that they all encoded the kinase domain of unc51-like kinase 1 (ULK1) (Fig. 1B). We next adopted co-immunoprecipitation (co-IP) to confirm the interaction between LRRK2 and ULK1 in mammalian cells. HEK293 cells were transfected with expression vectors encoding Flag epitope-tagged LRRK2 and HA epitope-tagged ULK1, either alone or in combination. Analysis of anti-Flag and anti-ULK1 immunoprecipitates derived from these cells revealed that the LRRK2 immunocomplexes specifically contained ULK1 and vice versa (Fig. 1C).

To determine which part of LRRK2 interacts with ULK1, we made different Flag-tagged deletion mutants of LRRK2 (Fig. 1A). Co-IP experiments reveal that LRRK2-C which includes the Roc-COR, kinase and WD40 domains, but not LRRK2-AL which encodes the Ank and LRR domains, interacts with ULK1 (Fig. 1D). We then examined LRRK2-MW which includes the kinase and WD40 domains and LRRK2-W which encodes the WD40 domain and observed that the WD40 domain itself could interact with ULK1 (Fig. 1E). We did co-IP of LRRK2 WD40 domain deletion mutant (LRRK2 ΔWD40) with ULK1 and found that full-length LRRK2, but not LRRK2 ΔWD40 could interact with ULK1, indicating that the WD40 of LRRK2 is essential for the interaction between LRRK2 and ULK1 (Fig. 1F).

ULK1 protein consists of an N-terminal kinase domain (KD) followed by a central proline/serine rich domain (PS) and a highly conserved carboxy-terminal domain (CTD) (Fig. 1B). To determine which part of ULK1 interacts with LRRK2, we made HA-tagged different domains of ULK1 and deletion mutants of ULK1 (Fig. 1B). Co-IP experiments revealed that only the kinase domain (KD) of ULK1 interacted with LRRK2 (Fig. 1G). On the other hand, deletion of the kinase domain abolished the ability of ULK1 to interact with LRRK2 (Fig. 1H). Taking together, our results indicate that LRRK2 interacts with ULK1 via the WD40 domain in LRRK2 and the kinase domain in ULK1.

Expression of LRRK2 leads to autophagosome formation

ULK1 has been recognized as a convergence point for multiple signals that control autophagy (Stephan and Herman, 2006; Kundu et al., 2008; Mizushima, 2010; Egan et al., 2011; Tamura et al., 2011; Itakura et al., 2012). Many studies indicate that LRRK2 especially those pathogenic mutants play a positive role in autophagy (Chen and Chan, 2009; Ramonet et al., 2011; Tamura et al., 2011; Wang et al., 2012; Itoh et al., 2013; Orenstein et al., 2013). However, discrepancy still exists in the function of LRRK2 in the autophagy-lysosome pathway (Manzoni, 2012). Since LRRK2 interacts with ULK1, we evaluated the role of LRRK2 in autophagy in different cell types including normal rat kidney (NRK), HeLa, HEK293 and cultured neurons. NRK cells stably expressing CFP-LC3 (hereafter termed as NRK-LC3 cells) were co-transfected with wild type or mutant forms of *LRRK2* and *RFP* (Red Fluorescent Protein, used as a transfection marker) expressing vectors. There were significantly more CFP-LC3 dots (indicator of autophagosome) in cells transfected with WT LRRK2 or the pathogenic G2019S mutant than control (Fig. 2A and 2B). Expression of the kinase dead form of LRRK2 (LRRK2 K1906M) did not induce the formation of autophagosome very significantly. In addition, expression of WT LRRK2 and G2019S mutant also induced the

 © Higher Education Press and Springer-Verlag Berlin Heidelberg 2013

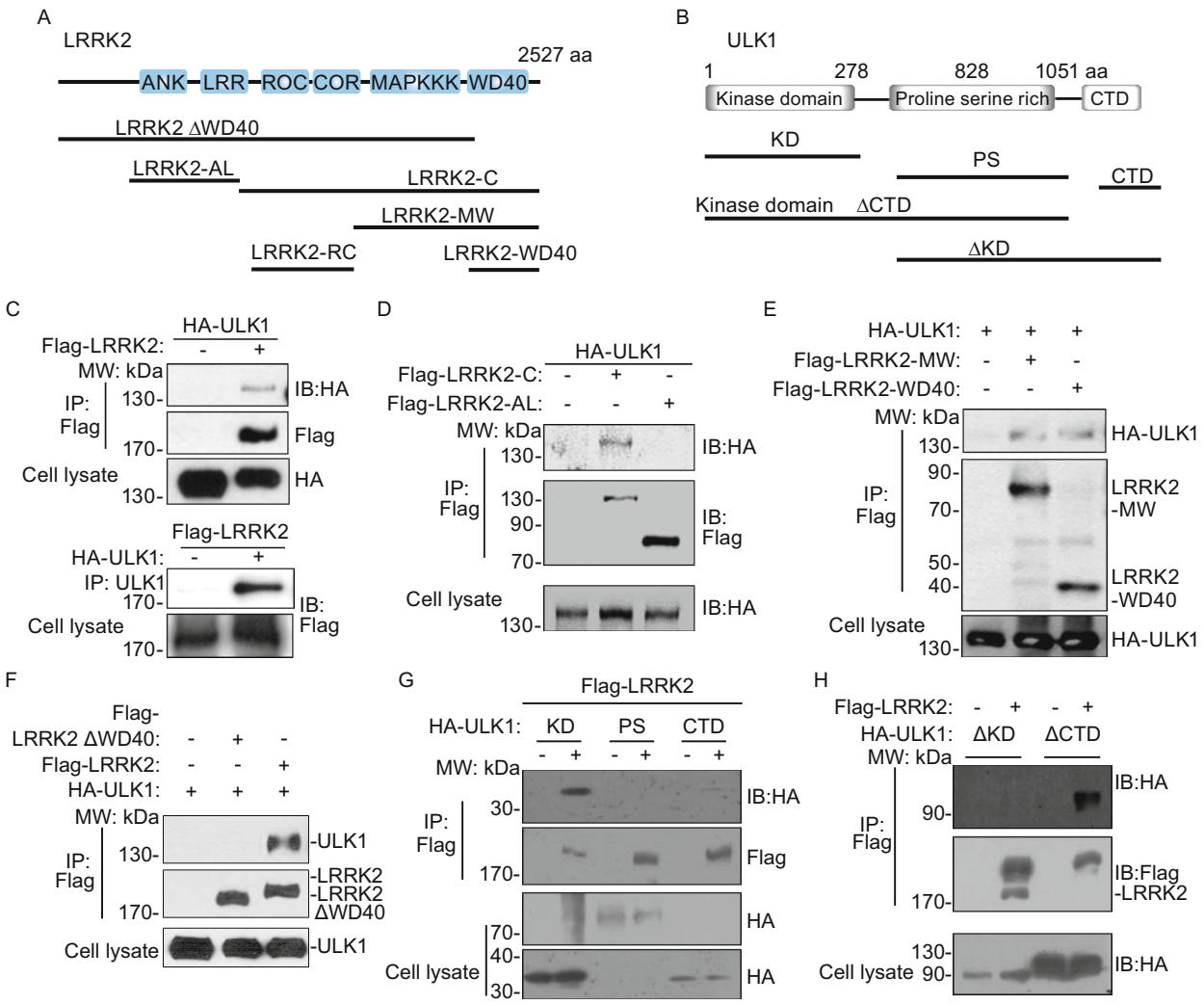

Figure 1. LRRK2 interacts with ULK1. (A and B) Schematic representation of functional domains of LRRK2 (A) and ULK1 (B). (C) ULK1 interacts with LRRK2 in cells. HEK293 cells were transfected with expression vectors encoding Flag-*LRRK2* and HA-*ULK1*, either alone or in combination. 36 h later, cell lysates were immunoprecipitated with anti-Flag or ULK1 antibody. Cell lysates and the immunocomplex were probed with anti-Flag (for LRRK2) and anti-HA (for ULK1) antibodies. (D–H). LRRK2 interacts with ULK1 via the WD40 domain of LRRK2 and the kinase domain of ULK1. Full length *ULK1*, *LRRK2* and their deletion mutants were transfected in HEK293 cells and analyzed as in (C). (D) ULK1 interacts with the C-terminal two-third of LRRK2. (E) ULK1 interacts with the WD40 domain of LRRK2. (F) WD40 domain of LRRK2 is essential for the interaction between LRRK2 and ULK1. (G) Kinase domain (KD) of ULK1 can interact with LRRK2. (H) Kinase domain of ULK1 is essential for the interaction between LRRK2 and ULK1. All experiments were repeated at least once and similar results were obtained.

accumulation of endogenous lipidated form of LC3 (LC3-II, an indicator of macroautophagy) in HEK293 cells (Fig. 2C and 2D). The boost of LC3-II levels were more obviously in the presence of leupeptin, an inhibitor of protease and autophagy. Interestingly, G2019S mutant induced the much higher level of LC3-II than wt LRRK2 and LRRK2 K1906M (Fig. 2C and 2D), corresponding to the induction of autophagosome formation in NRK-LC3 cells. Furthermore, over-expressed LRRK2 and LC3 co-localize with each other in U2OS cells undergoing starvation (Fig. S1).

We also confirmed the induction of autophagosome formation by transfection of TD2 (tdimer2) fused LRRK2 and LRRK2 G2019S in NRK-LC3 cells and HeLa cells stably expressing CFP-LC3 (HeLa-LC3 cells) (Figs. 2E and 3A). Since the WD40 domain in LRRK2 is required for its interaction with ULK1, we made the deletion mutants and found that they were no longer able to induce significant autophagosome formation (Figs. 2E, 2F and 3). The above results indicate that expression of LRRK2, especially LRRK2 G2019S mutant, can induce autophagy which is very likely to depend on the interaction between LRRK2 and ULK1.

© Higher Education Press and Springer-Verlag Berlin Heidelberg 2013

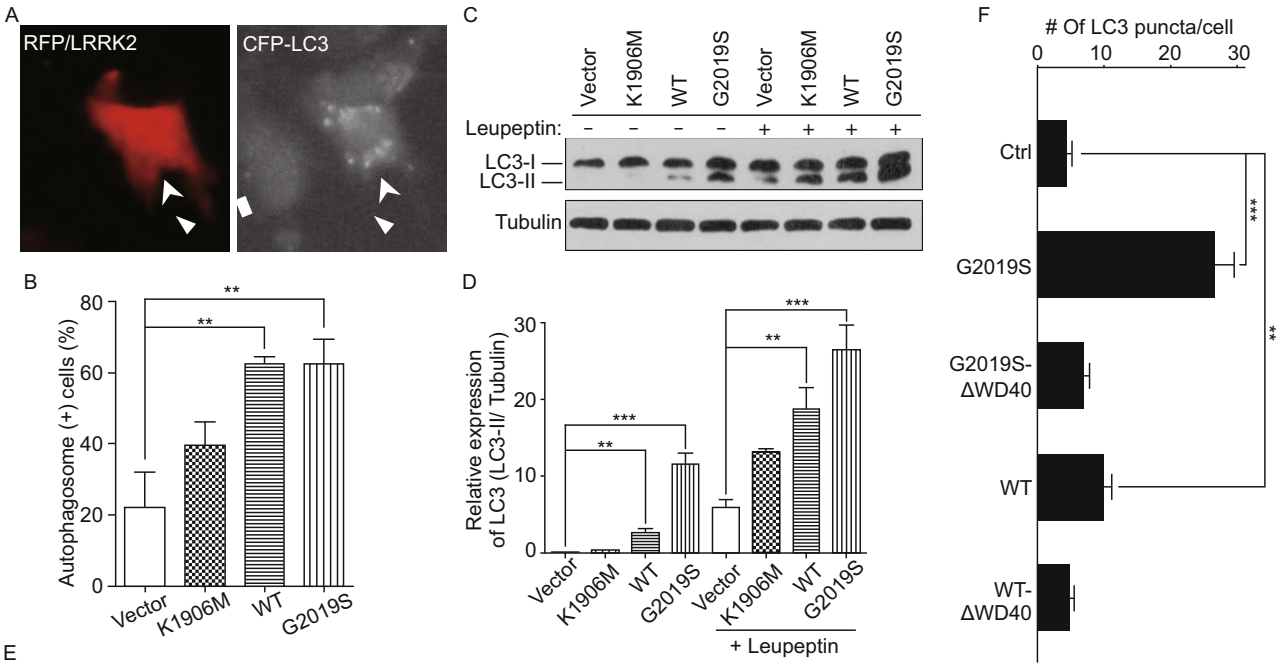

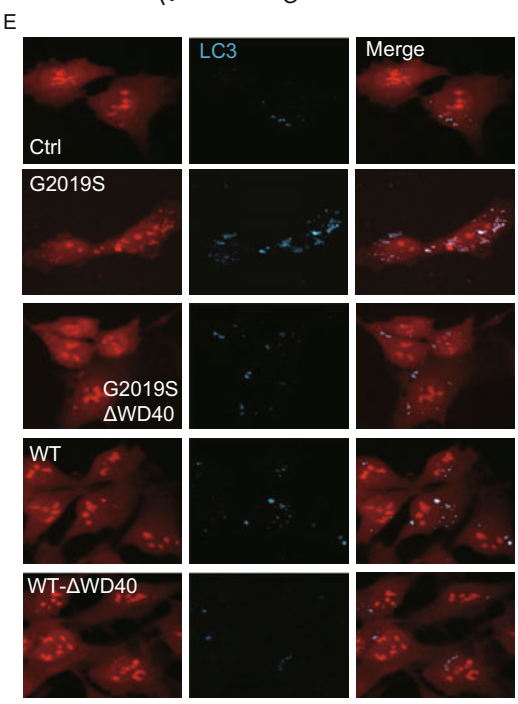

Figure 2. Expression of LRRK2 induces autophagy. (A and B) LRRK2 expression induces the formation of autophagosome. NRK cells stably expressing CFP-LC3 were transfected with empty vector, wild-type, kinase dead (K906M) or LRRK2 G2019S mutant together with RFP (Red Fluorescent Protein, marker for transfected cell). 36 h after transfection, autophagosome were analyzed and quantified by fluorescence microscopy. (A) A representative field showing a cell transfected with LRRK2 WT (arrow) and an untransfected cell (arrowhead). (B) Quantification of autophagosome positive cells. Values are means from 3 independent experiments ± SEM. For each group, more than 500 cells transfected from 3 experiments were quantified. (C) LRRK2 expression induces the conversion of endogenous LC3-I to LC3-II. HEK293 cells were transfected with different constructs as in (A) with or without leupeptin treatment. The levels of LC3-I or LC3-II were determined by Western blotting using LC3 antiserum. (D) Quantification of LC3-II levels normalized with Tubulin levels. Values are means from 3 independent experiments in (C) ± SEM. (E and F) WD40 domain is required for LRRK2 expression induced autophagy. NRK CFP-LC3 cells were transfected with empty vector, LRRK2 G2019S, LRRK2 G2019S ΔWD40, WT LRRK2 or LRRK2 ΔWD40. 36 h after transfection, autophagosome were analyzed and quantified with confocal microscope and Imaris software. (E) Representative field showing expression of LRRK2 G2019S and WT LRRK2 but not their WD40 deletion mutants can induce autophagosome formation. (F) Quantification of LC3 positive puncta in cells. Values are means ± SEM. For each group, >50 transfected cells from 3 experiments were quantified.

Expression of LRRK2 G2019S induces the loss of mitochondria and it can be rescued by knockdown of ULK1

We have shown previously that co-expression of LRRK2 G2019S and DLP1 induces dramatic clearance of mitochondria in HeLa cells (Niu et al., 2012), implicating that LRRK2 may play a role in mitophagy. Here, we inspected the role of LRRK2 without co-expression of DLP1. As shown in Fig. 3A, wt LRRK2, LRRK2 G2019S and LRRK2 G2019S ΔWD40 were co-localized with mitochondria and were able to induce mitochondrial fission as we have shown previously in HeLa-LC3 cells. Interestingly, only expression of LRRK2 G2019S could lead to significant decrease of mitochondrial number (Fig. 3). In addition, many of the LRRK2 G2019S protein and fragmented mitochondria co-localized with LC3 puncta, indicating the induction of mitophagy in HeLa-LC3 cells (Fig. 3A). Interestingly, although expression of wt LRRK2 or LRRK2

 © Higher Education Press and Springer-Verlag Berlin Heidelberg 2013

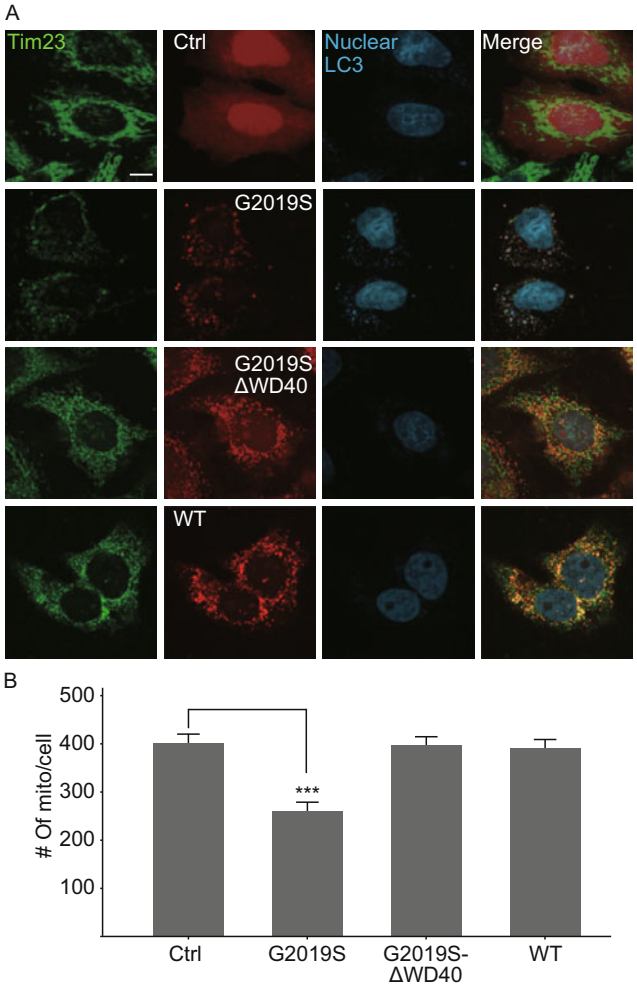

Figure 3. Expression of LRRK2 induces the fragmentation and reduction of mitochondria number in HeLa. HeLa-LC3 cells were transfected with empty vector, TD2-LRRK2 G2019S, TD2-LRRK2 G2019SΔWD40, or TD2-LRRK2 WT. 36 h after transfection, cells were fixed and stained with Tim23 (an inner membrane protein of mitochondria) for mitochondria (green), DAPI for nuclei (blue). Autophagosome was shown as blue LC3 dots. Mitochondria and LC3 dots were analyzed by confocal microscopy. (A) Expression of WT and LRRK2 G2019S promotes autophagosome formation and only expression of LRRK2 G2019S induces mitochondria clearance. (B) Quantification of the number of mitochondria in cells. Values are means ± SEM. For each group, >50 transfected cells from 3 experiments were quantified.

G2019S ΔWD40 were able to induce mitochondrial fission, there was no apparent loss of mitochondria (Fig. 3A).

To investigate whether LRRK2 plays a role in mitophagy in neurons, we adopted BacMam virus for more efficient transfection and for the reduction of potential overexpression-induced artifact. As shown in Fig. 4A and 4B, expression of the pathogenic LRRK2 G2019S mutant induced dramatic drop of mitochondria number in cortical neurons (~45/neuron vs. ~108/neuron for the control). Similar to that in HeLa-LC3 cells, WT LRRK2 did not induce significant decrease of mitochondria number (Fig. 3A and 3B).

ULK1 plays an essential role in mitophagy (Kundu et al., 2008; Egan et al., 2011) and we have shown above that the WD40 domain in LRRK2 is required for the interaction between LRRK2 and ULK1 and induction of autophagy by LRRK2. We postulated that ULK1 might play a role in LRRK2 G2019S induced mitophagy. To test this hypothesis, we tried to knock down the expression of ULK1 with shRNAs in LRRK2 G2019S expressing cells. Since it is hard to infect culture neurons with BacMam virus and transfect them with shRNAs at the same time, we did the analysis in NRK cells. We screened different ULK1 shRNAs and confirmed two of them that are capable of knocking down the levels of ULK1 efficiently (Fig. 4C). As shown in Fig. 4D, expression of LRRK2 G2019S induced dramatic decrease of mitochondria number or even clearance of mitochondria compared with the controls. Knockdown of ULK1 substantially suppressed the loss of mitochondria. However, we noticed the existence of fragmented mitochondria in those cells (Fig. 4D). This suggests that ULK1 knockdown could suppress LRRK2 G2019S expression-induced mitophagy but not mitochondrial fission.

Knockdown of DLP1 suppresses mitochondria clearance induced by LRRK2 G2019S

We and others have shown previously that DLP1 plays an essential role in LRRK2-induced mitochondrial fission (Niu et al., 2012; Wang et al., 2012). We went on to explore the possibility that LRRK2 G2019S expression induces mitochondrial fission through DLP1 and thereafter leads to mitochondria clearance. NRK cells transfected with control or shDLP1 expression vector were infected with control or LRRK2 G2019S expressing virus. Mitochondrial fission was noticed at around 16 h after LRRK2 G2019S expression (data not shown) and obvious mitochondria clearance was found around 24 h after infection (Fig. 5). However, mitochondria clearance was suppressed apparently in LRRK2 G2019S expressing cells transfected with shDLP1 (Fig. 5). Therefore, DLP1 is likely to play a role not only in mitochondrial fission, but also in mitochondria clearance.

LRRK2 interacts with MKK4/7, JIP3 to induce the activation of JNK synergistically

Despite the finding of interaction between LRRK2 and components of the JNK pathway similar to that of the MLK family, the role of LRRK2 in JNK signaling is still uncertain (Berwick and Harvey, 2011). To elucidate whether LRRK2 functions similarly to that of MLKs, we did co-immunoprecipitation of LRRK2 from brain cell lysate of *Flag-LRRK2* transgenic mice (Li et al., 2010) with Flag antibody. In this way, we could avoid the potential artificial effect generated by over-expression of individual proteins. The immunocomplexes were analyzed for the presence of endogenous JNK pathway components and revealed that LRRK2 interacts with MKK4, MKK7 and the scaffold protein, JIP3 (Fig. 6A–C), but not apparently with JNKs and the scaf-

© Higher Education Press and Springer-Verlag Berlin Heidelberg 2013

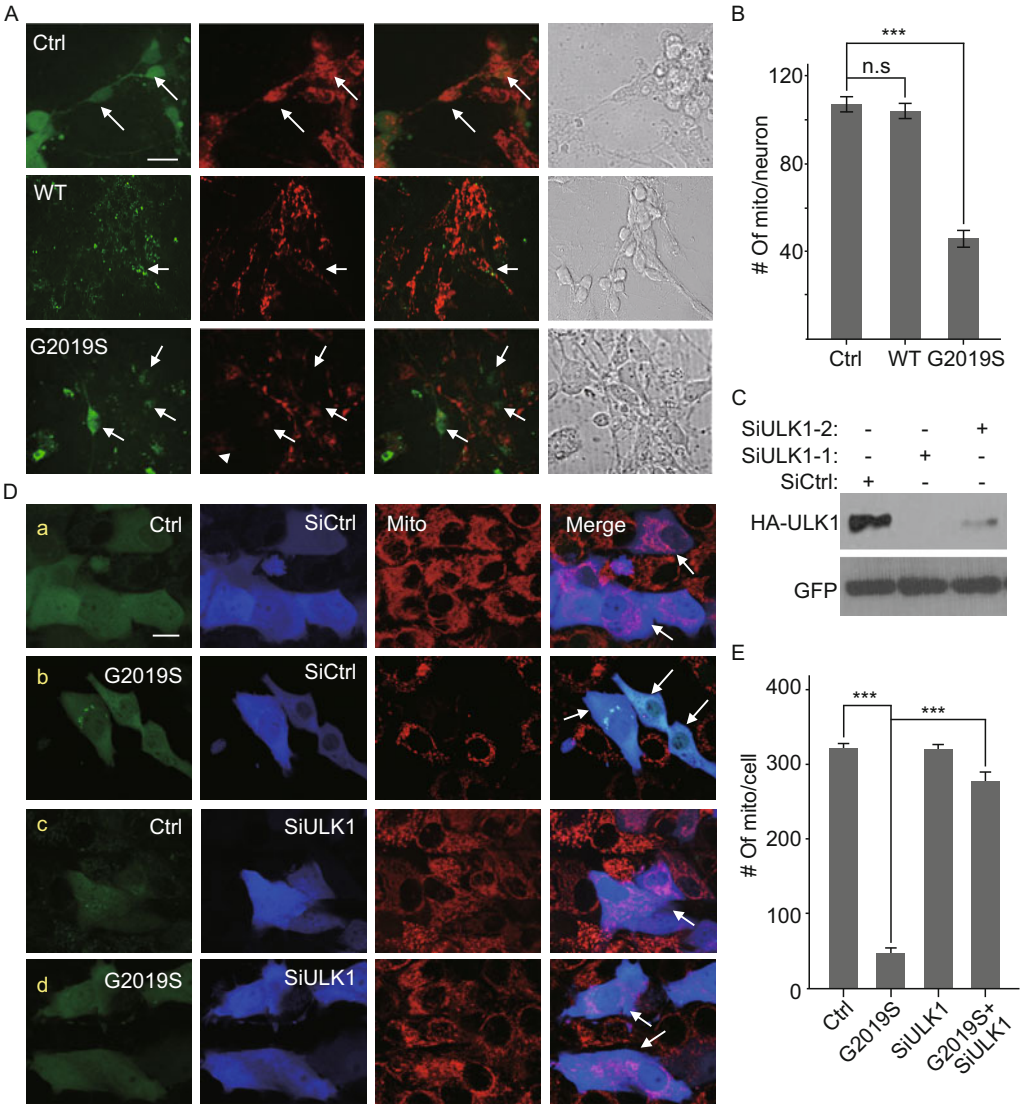

Figure 4. Expression of LRRK2 G2019S induces the reduction of mitochondria number in cortical neurons and it can be suppressed by ULK1 knockdown. (A) LRRK2 G2019S expression induces the loss of mitochondria in cortical neurons. 2 day *in vitro* cultured primary cortical neurons were infected with BacMam_LRRK2 WT_GFP, BacMam_LRRK2 G2019S_GFP or BacMam GFP separately for the expression of GFP-fused proteins. 40 h later, mitochondria were labeled with mitotracker deepred (20 nmol/L) and analyzed with DeltaVision living cell system. (B) Quantification of mitochondria numbers. Values are means ± SEM. n.s, $P > 0.05$, ***$P < 0.001$, 1-way ANOVA. 50 infected neurons from 3 independent experiments were counted for each group. (C) Screen of small hairpin constructs capable of ULK1 knockdown. HEK293 cells were transfected with HA-ULK1 together with scrambled (Ctrl) or shRNAs targeting ULK1. 72 h after transfection, cell lysates were analyzed by immunoblotting with anti-HA antiserum. GFP was used as a transfection efficiency control. The experiments were repeated once and similar results were obtained. (D) LRRK2 G2019S expression induces mitochondria clearance and it can be suppressed by knockdown of ULK1. NRK cells were transfected with control (a, c) or ULK1 (b,d) shRNAs (Blue). 16 h later, cells were infected with BacMam_LRRK2 G2019S_GFP (Green) as indicated. About 20 h after infection, cells were stained with MitoTracker deepred (Red) for mitochondria and the images were captured by confocal microscope. Bar = 10 μm. (E) Quantification of mitochondria in cells. Values are means ± SEM. ***$P < 0.001$, 1-way ANOVA. 50 cells from 3 independent experiments that were both transfected and infected were counted for each group.

fold proteins, POSH and JIP1 (data not shown). This implies that LRRK2 can form a complex with MKK4/7 and JIP3.

In order to determine whether LRRK2 acts as a MKKK, HEK293T cells were transfected with LRRK2, LRRK2 G2019S, MKK4, MKK7 and JIP3, either alone or in combination. As shown in Fig. 6D, expression of LRRK2 or LRRK2 G2019S induced the phosphorylation of JNKs indicating the activation of the JNK pathway. LRRK2 G2019S seemed to be

 © Higher Education Press and Springer-Verlag Berlin Heidelberg 2013

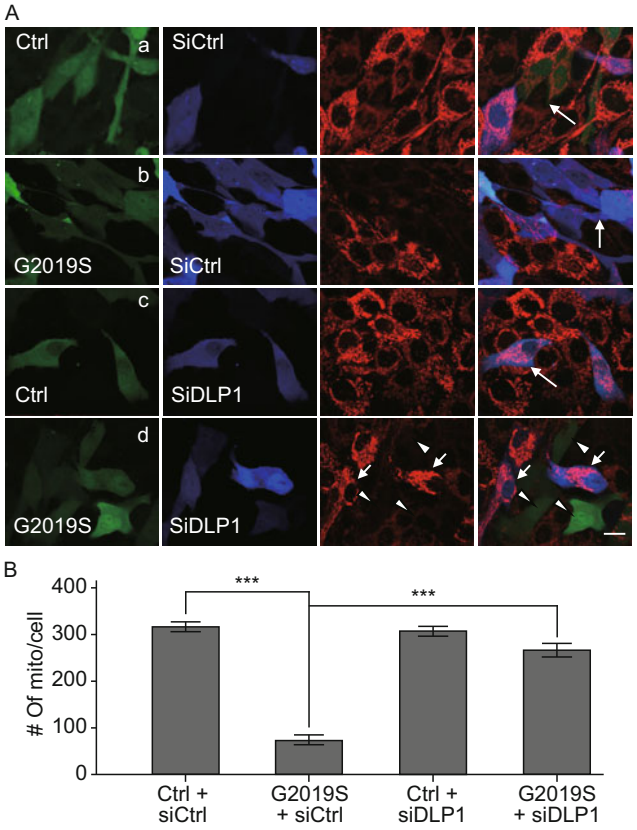

Figure 5. DLP1 depletion suppresses mitochondrial clearance induced by LRRK2 G2019S expression. (A) NRK cells were transfected with control (a and c) or DLP1 (b and d) shRNA (Blue), infected with virus and inspected as in Fig. 3D. Some cells infected with virus and transfected with shRNA were labeled with arrows (a–d) while some cells infected with LRRK2 G2019S expressing virus but not transfected with shRNA DLP1 were labeled with arrow head (d). Bar = 10 μm. (B) Quantification of mitochondria in cells. Values are means ± SEM. ***P < 0.001, 1-way ANOVA. 50 cells from 3 independent experiments that were both transfected and infected were counted for each group.

more effective in the induction. Interestingly, co-expression of LRRK2 or LRRK2 G2019S with MKK4 was more effective in the activation of JNKs (Fig. 6D). Similar results were obtained when LRRK2 or LRRK2 G2019S were co-expressed with JIP3 or MKK7 (Fig. 6E and 6F and data not shown). These results suggest that LRRK2 plays a similar role in the JNK pathway as MKKK and there is likely a synergistic effect between LRRK2 and MKK4/7 and JIP3 in the activation of JNK.

LRRK2 G2019S induced mitochondria clearance can be suppressed by inhibition of JNK activity

Mitochondrial function and mitophagy are influenced by proapoptotic signal transduction through the JNK pathway (Tournier et al., 2000). We therefore explored whether LRRK2 G2019S expression incurred JNK activation plays a role in the clearance of mitochondria. We infected cultured cortical neurons with LRRK2 G2019S expressing virus and analyzed the number of mitochondria both in the presence or absence of selective or specific JNK inhibitors. To minimize the potential nonspecific effect of JNK inhibitors, we tried 3 different kinds of JNK inhibitors, Sp600125, Quinazoline 13a (Q13a), and HIV-tag-JNK inhibitor I (JNK inhibitor I). Compared with SP600125, JNK inhibitor I is regarded as a highly specific JNK inhibitor, which does not inhibit the activity of ERK, protein kinase C or p38 at 500 μmol/L (Borsello et al., 2003). Recently, Q13a was found to be a potent JNK inhibitor (IC50 = 40 nmol/L), with >500-fold selectivity over p38 (He et al., 2011). As shown in Fig. 7, the loss of mitochondria incurred by LRRK2 G2019S expression could be substantially suppressed by different JNK inhibitors especially by Q13a and JNK inhibitor I. This implies that LRRK2 G2019S is likely to induce clearance of mitochondria through the activation of JNK.

DISCUSSION

Mitochondrial dysfunction has long been implicated in the etiopathogenesis of PD (Dagda et al., 2009; Exner et al., 2012). In this study, we identified a novel LRRK2 interacting protein, ULK1. In addition, we found that LRRK2 interacts with the endogenous MKK4, MKK7 and JIP3, and they are able to induce the activation of JNK synergistically. Expression of LRRK2 G2019S induces mitochondrial clearance and it is dependent on JNK, DLP1 and ULK1 respectively. This indicates that the JNK and the mitophagy signaling pathways may contribute to the neuronal dysfunction induced by LRRK2 G2019S.

Autophagy including mitophagy is primarily a protective process in response to cellular stresses; however, compromised mitochondrial clearance through mitophagy is also associated with cell death and PD etiopathogenesis (Levine and Kroemer, 2008; Springer and Kahle, 2011; Santos and Cardoso, 2012). Therefore, manipulation of autophagy has been proposed for the treatment of neurodegenerative disease (Springer and Kahle, 2011; Harris and Rubinsztein, 2012). More and more evidence are emerging that the autophagy process is altered in *LRRK2* PD models. However, whether LRRK2 plays a positive or a negative role in the autophagy-lysosome pathway is still not conclusive. Most studies showed accumulation of autophagosomes after overexpression of wild-type LRRK2, G2019S or LRRK2 R1441C mutants in various cell lines and transgenic mice (Chen and Chan, 2009; Ramonet et al., 2011; Tamura et al., 2011; Wang et al., 2012; Itoh et al., 2013). *LRRK2*-knockout mice displayed a biphasic alteration in autophagy that first increased in young mice and then decreased with age (Tong and Shen, 2012). Knockdown of LRRK2 with siRNA led to increased autophagic activity (Alegre-Abarrategui and Wade-Martins, 2009). However, it was shown recently that G2019S mutant fibroblasts exhibited higher autophagic activity levels than control fibroblasts (Bravo-San Pedro et al., 2013). We have confirmed that expression of wild-type or LRRK2 G2019S in different cell lines induced the elevation of LC3-II

© Higher Education Press and Springer-Verlag Berlin Heidelberg 2013

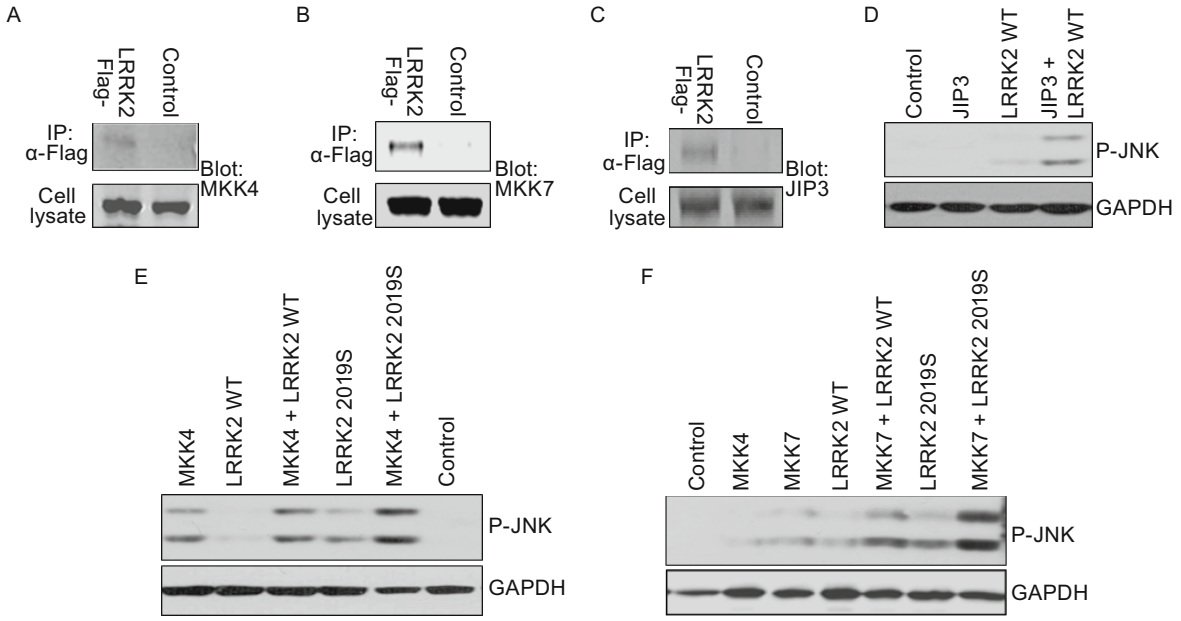

Figure 6. LRRK2 interacts with MKK4/7, JIP3 and coordinates with them in the activation of JNK. (A–C) Cell lysates from brains of *Flag-LRRK2* transgenic mouse were immunoprecipitated with anti-Flag beads and the immunocomplexes were analyzed for the MKK4 (A), MKK7 (B) and JIP3 (C). (D–F). Empty vector, LRRK2 WT, LRRK2 G2019S and MKK4 (D), MKK7 (E), and JIP3 (F) were transfected either alone or together in HEK 293 cells as indicated. 24 h later, the levels of JNK activity were determined by Western blotting with antibody for the phosphorylated JNK (P-JNK). GAPDH was used as a loading control. All experiments were repeated at least once and similar results were obtained.

levels as well as the formation of autophagosomes.

Autophagic and mitochondrial abnormalities have been observed in the brains of aged LRRK2 G2019S transgenic mice (Ramonet et al., 2011) and depletion of dendritic mitochondria in neurons expressing LRRK2 G2019S has been reported during the preparation of this manuscript (Itoh et al., 2013). We provided evidence here that expression of LRRK2 G2019S but not wt LRRK2 can induce the apparent clearance of mitochondria in cortical neurons including the soma. The induction of LC3-II and formation of autophagosomes co-localized with fragmented mitochondria indicates that expression of LRRK2 G2019S is very likely to stimulate the clearance of mitochondria through autophagy.

ULK1 is required for autophagy and has been recognized as a critical regulator of autophagy and mitophagy (Kundu et al., 2008; Egan et al., 2011; Itakura et al., 2012). We discovered ULK1 as a novel LRRK2 interacting protein and confirmed that the interaction between LRRK2 and ULK1 depends on the WD40 domain of LRRK2 and the kinase domain of ULK1 respectively. Interestingly, expression of LRRK2 G2019S with deletion of WD40 domain could not induce the formation of autophagosomes and mitophagy although it still caused mitochondrial fission. This indicates that the interaction between LRRK2 and ULK1 is required for LRRK2 G2019S expression-incurred mitophagy. We showed further that depletion of ULK1 or DLP1 could suppress LRRK2 G2019S expression-induced mitochondria clearance. Fission is thought to be important for mitophagy because inhibition of division slows down mitophagy (Itoh et al., 2013). Since we and others have found that LRRK2 G2019S could induce mitochondrial fission through DLP1 (Niu et al., 2012; Wang et al., 2012) and ULK1 knockdown suppresses LRRK2 G2019S expression induced mitophagy but not apparently mitochondrial fission (this study), it is very likely that expression of LRRK2 G2019S induces mitochondrial fission via DLP1 and mitophagy through ULK1 afterward.

The effect of LRRK2 on JNK activity is still equivocal with most of the studies showing no effect or even suppression of JNK activity (Becker and Bonni, 2006; White et al., 2007; Hsu et al., 2010). However, West et al. have shown that LRRK2 overexpression activates JNK in SH-SY5Y cells independent of LRRK2 activity (West et al., 2007) and JNK phosphorylation level was found recently to be increased in the substantia nigra of *LRRK2 G2019S* transgenic mice (Chen et al., 2012). In this study, we found that Flag-LRRK2 expressed in transgenic mouse brain interacted with the endogenous MKK4 and MKK7, and JIP3, but not apparently with the JNK pathway scaffold protein POSH. This indicates that LRRK2 can form a complex with MKK4/7 and JIP3, different from the POSH-JIP apoptotic complex (PJAC) that we reported previously (Xu et al., 2005; Kukekov et al., 2006). The induction of higher level of JNK phosphorylation by LRRK2 G2019S than wt LRRK2 is in accordance with the gain-of-function role of LRRK2 G2019S in PD development. Interestingly, our results from co-expression indicate that there is synergistic effect in the activation of JNK

© Higher Education Press and Springer-Verlag Berlin Heidelberg 2013

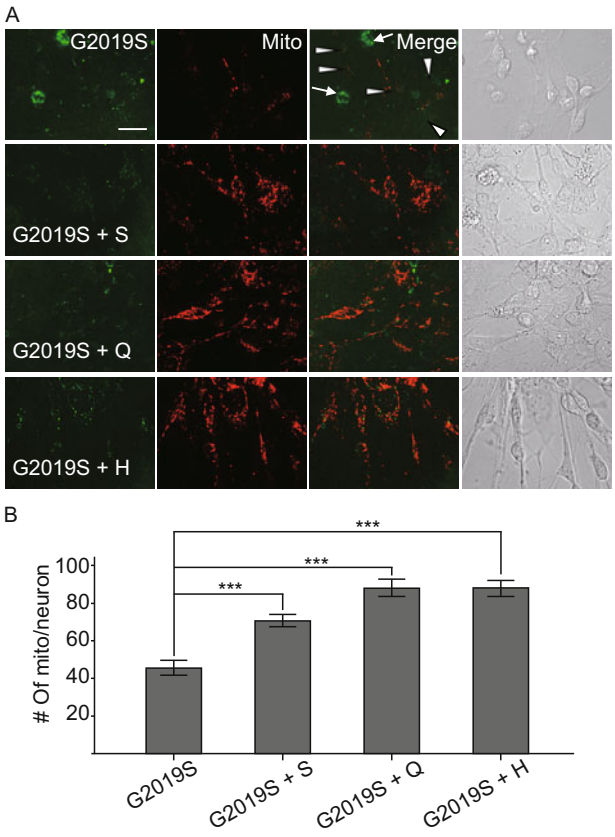

Figure 7. LRRK2 G2019S expression induced loss of mitochondria in cortical neurons can be suppressed by JNK inhibitors. (A) Cortical neurons were infected with BacMam_LRRK2 G2019S_GFP as in Fig. 3A. 32 h later, different JNK inhibitors, Sp600125 (S, 8 μmol/L), Q13a (Q, 30 nmol/L) or JNK inhibitor I (H, 6 μmol/L) were applied to the culture medium for 8 h. Mitochondria were detected as in Fig. 3A. Some cells infected with virus showing loss of mitochondria were labeled with arrow heads while two dying cells were labeled with arrow. Bar = 10 μm. (B) Quantification of mitochondria in neurons. Values are means ± SEM. ***P < 0.001, 1-way ANOVA. 50 infected neurons from 3 independent experiments were counted for each group.

between LRRK2 and MKK4/7 and JIP3, similar to that of MLKs (Xu et al., 2005). Together with the evidence that LRRK2 has a kinase domain homologous to other MKKKs and expression of LRRK2 is able to phosphorylate MKK4 and MKK7 (Gloeckner et al., 2009), it is now reasonable to recognize LRRK2 as a MKKK.

Inhibition of the JNK pathway has been proposed for therapeutic interventions in parkinsonian neurodegeneration (Kuan and Burke, 2005; Cui et al., 2007; Santos and Cardoso, 2012). We found that LRRK2 G2019S expression-incurred mitochondria loss could be suppressed significantly by 3 different kinds of selective or specific JNK inhibitors. This implies the involvement of JNK activation in LRRK2 G2019S induced clearance of mitochondria, in agreement with previous findings that mitochondrial function and mitophagy are influenced by the JNK pathway (Tournier et al., 2000).

In this study, we provide evidence that LRRK2 G2019S expression induces mitophagy and it can be suppressed by inhibition of JNK activity and knockdown of either ULK1 or DLP1. It is reasonable to assume that expression of LRRK2 G2019S would lead to the activation of JNKs and the dysfunction of mitochondria. Dysfunction of mitochondria would lead to the recruitment of DLP1 to mitochondria to induce mitochondrial fission and subsequently mitophagy through a ULK1 dependent pathway. Currently, we are unable to exclude the possibility that LRRK2 may induce the mitochondrial dysfunction and recruit DLP1 to mitochondria at the same time. It will be intriguing to investigate in the future the detailed relationship between JNK activation, DLP1 translocation and the activation of ULK1. Nevertheless, our study may give rise to potential novel therapeutic strategies for PD.

MATERIALS AND METHODS

Materials

LC3 and Flag antibodies, Flag agrose beads, Sp600125 and HIV-tag-JNK inhibitor I were purchased from Sigma; monoclonal LRRK2 antibody was purchased from EPITOMICS (Catalog # 3515-1). Myc tag monoclonal antibody was from MBL Ltd; Mouse GFP (clone B-2), JIP3, Tim23 and GAPDH antibody were from Santa Cruz. Antibodies for MKK4, MKK7 and phosphorylated JNK were purchased from Cell Signaling Inc. Q13a was kindly provided by Dr. Philip V. LoGrasso. BacMam virus encoding full-length LRRK2 (BacMam_LRRK2 WT_GFP), G2019S mutant (BacMam_LRRK2 G2019S_GFP) or control (BacMam GFP) were purchased from Invitrogen.

Constructs

Full-length (FL) *LRRK2 WT*, *G2019S*, *Kinase-Dead* (*KD*), TD2-*LRRK2 WT*, and TD2-*LRRK2 G2019S*, *Flag-LRRK2-M* (aa672–1889), *Flag-LRRK2-C* (aa1213–2527), *Flag-ANK-LRR* (aa672–1267), and *Flag-ROC-COR* (aa1213–1889) in pcDNA3.1 (Invitrogen) were described previously (Niu et al., 2012). Flag-*LRRK2 ΔWD40* (aa1–2138), *MAP-KKK-WD40* (aa1878–2527), *WD40* (aa2141–2500), TD2-*LRRK2 WT ΔWD40* (aa1–2138) and TD2-*LRRK2 G2019S ΔWD40* (aa1–2138), were PCR amplified from FL *LRRK2 WT* constructs or TD2-*LRRK2 WT* or TD2-*LRRK2 G2019S* and subcloned into pcDNA3.1. HA-ULK1, HA-hAtg13, HA-FIP200 constructs were kind gifts from Dr. Noboru Mizushima in Tokyo Medical and Dental University, Japan. ULK1 deletion mutants were PCR amplified from HA-ULK1 constructs and subcloned into pcDNA3.1. The oligonucleotides for siULK1 were annealed and cloned into pSIREN-RetroQ-DsRed (BD Biosciences). The target sequences for ULK1 are ULK1-1: 5′-AGACTCCTGTGACACAGAT-3′ and ULK1-2: 5′-GTACCTCCAGAGCAACATG-3′. shDLP1 in pGCsi_U6NeoGFP were described previously (Niu et al., 2012). MKK4, MKK7 and JIP3 were kindly provided by Dr. R Davis.

Cell culture, transfection and infection

NRK (Normal Rat kidney) cells stably expressing LC3 were kind gifts from Dr. Li Yu in Tsinghua University, China. The primary cultures of cerebral cortex neurons were maintained as described previously (Xu et al., 2003; Niu et al., 2012). For baculovirus infection, 2 day *in vitro*

© Higher Education Press and Springer-Verlag Berlin Heidelberg 2013

(DIV) primary cultured cortical neurons were infected according to the manufacturer's instructions.

Co-immunoprecipitation assays and Western blotting

Mouse brains from three month-old Flag-LRRK2 transgenic and control mice were from Dr. Zhenyu Yue (Li et al., 2007). Co-immunoprecipitation and Western blotting were carried out as previously described (Xu et al., 2003).

Image acquisition and quantification

Fluorescent images were captured using a confocal microscope (ZEISS LSM700 or ZEISS Observer ZI) or DeltaVision Living cell system. Quantification of mitochondria in cells was done in a similar way as described previously (Rodriguez-Enriquez et al., 2009). Briefly, Mitotracker Deepred (Invitrogen) was added to culture medium to a final concentration of 50 nmol/L for 15 min and then two-third of the medium was replaced with fresh medium. Image stacks of Mitotracker Deep-red-loaded cells were collected at 1 μm intervals with a DeltaVision Living cell system. 20 random fields per condition were acquired using the 63× objective and representative images were shown. Mitochondria and LC3 puncta number was analyzed with Imaris ×64 software.

Statistical analyses

Results are presented as means ± SEM. Statistical significance was determined by comparing means of different groups using one-way ANOVA followed by Tukey's post hoc honestly significant difference test. $^{*}P < 0.05$; $^{**}P < 0.01$; $^{***}P < 0.001$.

ACKNOWLEDGEMENTS

We would like to thank Dr. L Yu for the advices for this study and Drs. Z Yue, M. Cookson, N Mizushima, L Yu, P LoGrasso, and R Davis for the valuable materials used in this manuscript. This work was supported by grants from the Chinese Academy of Sciences (XDA01010105), the National Natural Science Foundation of China (Grant Nos. 30725007, 31271156 and 31270826), and the National Basic Research Program (973 Program) (No. 2012CB517904).

ABBREVIATIONS

DLP1, dynamin like protein 1; JNK, c-Jun N-terminal kinase; LC3, microtubule-associated protein light chain 3; LRRK2, Leucine rich repeat kinase 2; MKK, mitogen-activated protein kinase kinase; PD, Parkinson's disease; ULK1, uncoordinated family member (unc) 51-like kinase 1

COMPLIANCE WITH ETHICS GUIDELINES

Yuangang Zhu, Chunyan Wang, Mei Yu, Jie Cui, Liang Liu and Zhiheng Xu declare that they have no conflict of interest.

All institutional and national guidelines for the care and use of laboratory animals were followed.

REFERENCES

Alegre-Abarrategui, J., and Wade-Martins, R. (2009). Parkinson disease, LRRK2 and the endocytic-autophagic pathway. Autophagy 5, 1208–1210.

Becker, E.B., and Bonni, A. (2006). Pin1 mediates neural-specific activation of the mitochondrial apoptotic machinery. Neuron 49, 655–662.

Berwick, D.C., and Harvey, K. (2011). LRRK2 signaling pathways: the key to unlocking neurodegeneration? Trends Cell Biol 21, 257–265.

Borsello, T., Clarke, P.G., Hirt, L., Vercelli, A., Repici, M., Schorderet, D.F., Bogousslavsky, J., and Bonny, C. (2003). A peptide inhibitor of c-Jun N-terminal kinase protects against excitotoxicity and cerebral ischemia. Nat Med 9, 1180–1186.

Bravo-San Pedro, J.M., Niso-Santano, M., Gomez-Sanchez, R., Pizarro-Estrella, E., Aiastui-Pujana, A., Gorostidi, A., Climent, V., Lopez de Maturana, R., Sanchez-Pernaute, R., Lopez de Munain, A., et al. (2013). The LRRK2 G2019S mutant exacerbates basal autophagy through activation of the MEK/ERK pathway. Cell Mol Life Sci 70, 121–136.

Chen, C.Y., Weng, Y.H., Chien, K.Y., Lin, K.J., Yeh, T.H., Cheng, Y.P., Lu, C.S., and Wang, H.L. (2012). (G2019S) LRRK2 activates MKK4-JNK pathway and causes degeneration of SN dopaminergic neurons in a transgenic mouse model of PD. Cell Death Differ 19, 1623–1633.

Chen, H., and Chan, D.C. (2009). Mitochondrial dynamics—fusion, fission, movement, and mitophagy—in neurodegenerative diseases. Hum Mol Genet 18, R169–176.

Cookson, M.R. (2010). The role of leucine-rich repeat kinase 2 (LRRK2) in Parkinson's disease. Nat Rev Neurosci 11, 791–797.

Cui, J., Yu, M., Niu, J., Yue, Z., and Xu, Z. (2011). Expression of Leucine-Rich Repeat Kinase 2 (LRRK2) Inhibits the Processing of uMtCK to Induce Cell Death in cell culture model system. Biosci Rep. (In Press).

Cui, J., Zhang, M., Zhang, Y.Q., and Xu, Z.H. (2007). JNK pathway: diseases and therapeutic potential. Acta Pharmacol Sin 28, 601–608.

Dagda, R.K., Zhu, J., and Chu, C.T. (2009). Mitochondrial kinases in Parkinson's disease: converging insights from neurotoxin and genetic models. Mitochondrion 9, 289–298.

Egan, D.F., Shackelford, D.B., Mihaylova, M.M., Gelino, S., Kohnz, R.A., Mair, W., Vasquez, D.S., Joshi, A., Gwinn, D.M., Taylor, R., et al. (2011). Phosphorylation of ULK1 (hATG1) by AMP-activated protein kinase connects energy sensing to mitophagy. Science 331, 456–461.

Exner, N., Lutz, A.K., Haass, C., and Winklhofer, K.F. (2012). Mitochondrial dysfunction in Parkinson's disease: molecular mechanisms and pathophysiological consequences. EMBO J 31, 3038–3062.

Friedman, L.G., Lachenmayer, M.L., Wang, J., He, L., Poulose, S.M., Komatsu, M., Holstein, G.R., and Yue, Z. (2012). Disrupted autophagy leads to dopaminergic axon and dendrite degeneration and promotes presynaptic accumulation of alpha-synuclein and LRRK2 in the brain. J Neurosci 32, 7585–7593.

Gloeckner, C.J., Schumacher, A., Boldt, K., and Ueffing, M. (2009). The Parkinson disease-associated protein kinase LRRK2 exhibits MAPKKK activity and phosphorylates MKK3/6 and MKK4/7, in vitro. J Neurochem 109, 959–968.

Greggio, E., Jain, S., Kingsbury, A., Bandopadhyay, R., Lewis, P., Kaganovich, A., van der Brug, M.P., Beilina, A., Blackinton, J., Thomas, K.J., et al. (2006). Kinase activity is required for the toxic effects of mutant LRRK2/dardarin. Neurobiol Dis 23, 329–341.

Harris, H., and Rubinsztein, D.C. (2012). Control of autophagy as a

© Higher Education Press and Springer-Verlag Berlin Heidelberg 2013

therapy for neurodegenerative disease. Nat Rev Neurol 8, 108–117.

He, Y., Kamenecka, T.M., Shin, Y., Song, X., Jiang, R., Noel, R., Duckett, D., Chen, W., Ling, Y.Y., Cameron, M.D., et al. (2011). Synthesis and SAR of novel quinazolines as potent and brain-penetrant c-jun N-terminal kinase (JNK) inhibitors. Bioorg Med Chem Lett 21, 1719–1723.

Hsu, C.H., Chan, D., and Wolozin, B. (2010). LRRK2 and the stress response: interaction with MKKs and JNK-interacting proteins. Neurodegener Dis 7, 68–75.

Itakura, E., Kishi-Itakura, C., Koyama-Honda, I., and Mizushima, N. (2012). Structures containing Atg9A and the ULK1 complex independently target depolarized mitochondria at initial stages of Parkin-mediated mitophagy. J Cell Sci 125, 1488–1499.

Itoh, K., Nakamura, K., Iijima, M., and Sesaki, H. (2013). Mitochondrial dynamics in neurodegeneration. Trends Cell Biol 23, 64–71.

Jankowski, M. (2007). [The role of JNK pathway in familial Parkinson's disease]. Postepy Biochem 53, 297–303.

Kuan, C.Y., and Burke, R.E. (2005). Targeting the JNK signaling pathway for stroke and Parkinson's diseases therapy. Curr Drug Targets CNS Neurol Disord 4, 63–67.

Kukekov, N.V., Xu, Z., and Greene, L.A. (2006). Direct interaction of the molecular scaffolds POSH and JIP is required for apoptotic activation of JNKs. J Biol Chem 281, 15517–15524.

Kumari, U., and Tan, E.K. (2009). LRRK2 in Parkinson's disease: genetic and clinical studies from patients. FEBS J 276, 6455–6463.

Kundu, M., Lindsten, T., Yang, C.Y., Wu, J., Zhao, F., Zhang, J., Selak, M.A., Ney, P.A., and Thompson, C.B. (2008). Ulk1 plays a critical role in the autophagic clearance of mitochondria and ribosomes during reticulocyte maturation. Blood 112, 1493–1502.

Levine, B., and Kroemer, G. (2008). Autophagy in the pathogenesis of disease. Cell 132, 27–42.

Li, X., Patel, J.C., Wang, J., Avshalumov, M.V., Nicholson, C., Buxbaum, J.D., Elder, G.A., Rice, M.E., and Yue, Z. (2010). Enhanced striatal dopamine transmission and motor performance with LRRK2 overexpression in mice is eliminated by familial Parkinson's disease mutation G2019S. J Neurosci 30, 1788–1797.

Li, X., Tan, Y.C., Poulose, S., Olanow, C.W., Huang, X.Y., and Yue, Z. (2007). Leucine-rich repeat kinase 2 (LRRK2)/PARK8 possesses GTPase activity that is altered in familial Parkinson's disease R1441C/G mutants. J Neurochem 103, 238–247.

Manzoni, C. (2012). LRRK2 and autophagy: a common pathway for disease. Biochem Soc Trans 40, 1147–1151.

Mizushima, N. (2010). The role of the Atg1/ULK1 complex in autophagy regulation. Curr Opin Cell Biol 22, 132–139.

Niu, J., Yu, M., Wang, C., and Xu, Z. (2012). Leucine-rich repeat kinase 2 disturbs mitochondrial dynamics via Dynamin-like protein. J Neurochem 122, 650–658.

Orenstein, S.J., Kuo, S.H., Tasset, I., Arias, E., Koga, H., Fernandez-Carasa, I., Cortes, E., Honig, L.S., Dauer, W., Consiglio, A., et al. (2013). Interplay of LRRK2 with chaperone-mediated autophagy. Nat Neurosci 16, 394–406.

Ramonet, D., Daher, J.P., Lin, B.M., Stafa, K., Kim, J., Banerjee, R., Westerlund, M., Pletnikova, O., Glauser, L., Yang, L., et al. (2011). Dopaminergic neuronal loss, reduced neurite complexity and autophagic abnormalities in transgenic mice expressing G2019S mutant LRRK2. PLoS One 6, e18568.

Rodriguez-Enriquez, S., Kai, Y., Maldonado, E., Currin, R.T., and Lemasters, J.J. (2009). Roles of mitophagy and the mitochondrial permeability transition in remodeling of cultured rat hepatocytes. Autophagy 5, 1099–1106.

Saha, S., Guillily, M.D., Ferree, A., Lanceta, J., Chan, D., Ghosh, J., Hsu, C.H., Segal, L., Raghavan, K., Matsumoto, K., et al. (2009). LRRK2 modulates vulnerability to mitochondrial dysfunction in Caenorhabditis elegans. J Neurosci 29, 9210–9218.

Santos, D., and Cardoso, S.M. (2012). Mitochondrial dynamics and neuronal fate in Parkinson's disease. Mitochondrion 12, 428–437.

Springer, W., and Kahle, P.J. (2011). Regulation of PINK1-Parkin-mediated mitophagy. Autophagy 7, 266–278.

Stephan, J.S., and Herman, P.K. (2006). The regulation of autophagy in eukaryotic cells: do all roads pass through Atg1? Autophagy 2, 146–148.

Tamura, Y., Itoh, K., and Sesaki, H. (2011). SnapShot: Mitochondrial dynamics. Cell 145, 1158, 1158.e1.

Tong, Y., and Shen, J. (2012). Genetic analysis of Parkinson's disease-linked leucine-rich repeat kinase 2. Biochem Soc Trans 40, 1042–1046.

Tournier, C., Hess, P., Yang, D.D., Xu, J., Turner, T.K., Nimnual, A., Bar-Sagi, D., Jones, S.N., Flavell, R.A., and Davis, R.J. (2000). Requirement of JNK for stress-induced activation of the cytochrome c-mediated death pathway. Science 288, 870–874.

Wang, X., Yan, M.H., Fujioka, H., Liu, J., Wilson-Delfosse, A., Chen, S.G., Perry, G., Casadesus, G., and Zhu, X. (2012). LRRK2 regulates mitochondrial dynamics and function through direct interaction with DLP1. Hum Mol Genet 21, 1931–1944.

West, A.B., Moore, D.J., Biskup, S., Bugayenko, A., Smith, W.W., Ross, C.A., Dawson, V.L., and Dawson, T.M. (2005). Parkinson's disease-associated mutations in leucine-rich repeat kinase 2 augment kinase activity. Proc Natl Acad Sci U S A 102, 16842–16847.

West, A.B., Moore, D.J., Choi, C., Andrabi, S.A., Li, X., Dikeman, D., Biskup, S., Zhang, Z., Lim, K.L., Dawson, V.L., et al. (2007). Parkinson's disease-associated mutations in LRRK2 link enhanced GTP-binding and kinase activities to neuronal toxicity. Hum Mol Genet 16, 223–232.

White, L.R., Toft, M., Kvam, S.N., Farrer, M.J., and Aasly, J.O. (2007). MAPK-pathway activity, Lrrk2 G2019S, and Parkinson's disease. J Neurosci Res 85, 1288–1294.

Xu, Z., Kukekov, N.V., and Greene, L.A. (2003). POSH acts as a scaffold for a multiprotein complex that mediates JNK activation in apoptosis. EMBO J 22, 252–261.

Xu, Z., Kukekov, N.V., and Greene, L.A. (2005). Regulation of apoptotic c-Jun N-terminal kinase signaling by a stabilization-based feedforward loop. Mol Cell Biol 25, 9949–9959.

Xu, Z., Maroney, A.C., Dobrzanski, P., Kukekov, N.V., and Greene, L.A. (2001). The MLK family mediates c-Jun N-terminal kinase activation in neuronal apoptosis. Mol Cell Biol 21, 4713–4724.

© Higher Education Press and Springer-Verlag Berlin Heidelberg 2013